







BIOSURFACTANT-INDUCED PER- AND POLYFLUOROALKYL LEACHING FROM AQUEOUS FILM-FORMING FOAM IMPACTED SOIL

Sophie R. Hibben¹ , Alraune Zech² , Bas van der Grift³ , Jacco Koekoek⁴ , Sicco Brandsma⁴ , Johan van Leeuwen^{1,3} 

¹Utrecht University, Department of Earth Sciences, Utrecht, The Netherlands; ²Utrecht University, Faculty of Geosciences, Utrecht, The Netherlands; ³KWR Water Research Institute, Nieuwegein, The Netherlands; ⁴Vrije Universiteit Amsterdam, Department of Environment and Health, Amsterdam, The Netherlands

Correspondence to:

Alraune Zech,
a.zech@uu.nl

How to Cite:

Hibben, S., Zech, A., van der Grift, B., Koekoek, J., Brandsma, S., & van Leeuwen, J. (2025). Biosurfactant-Induced PFAS Leaching from Aqueous Film-Forming Foam (AFFF) Impacted Soil. *InterPore Journal*, 2(4), IPJ011225-4. <https://doi.org/10.69631/7v8xmn98>

RECEIVED: 19 Dec. 2024

ACCEPTED: 15 Aug. 2025

PUBLISHED: 1 Dec. 2025

ABSTRACT

The development of sustainable per- and polyfluoroalkyl (PFAS) remediation techniques is critical for the removal of contaminants from soil and water at sites impacted by aqueous film-forming foam (AFFF). This study is the first to explore the feasibility of flushing PFAS with a rhamnolipid biosurfactant solution using column testing and soil from an AFFF-contaminated site. Soil was flushed by either tap water alone or a 0.005% rhamnolipid solution. The PFAS concentrations in eluate and mass balances were compared for each test. In the first 12 pore volumes, 91% of the total perfluorooctane sulfonic acid (PFOS) flushed by the rhamnolipid solution was removed, while only 64% of PFOS was flushed in that time by tap water alone. Phosphate leached from soil and PFOS measured in the same eluate had similar concentration patterns, suggesting competitive sorption occurs with negatively charged phosphate, PFOS, and the anionic biosurfactant rhamnolipid. The flushing tests also show that there is no significant difference in flushing with a biosurfactant for PFAS compounds other than PFOS. Transport modeling confirmed that PFOS retardation (R-value) was lower with the rhamnolipid solution ($R = 9.76$) than with tap water ($R = 22.3$), which indicates that it is more efficient at removing PFOS from soil than water alone. This concept study provides insight into the release of PFAS compounds from a real contaminated saturated soil containing organic carbon, clay, and a complex mixture of PFAS. It shows promising first results for the use of biosurfactants as a sustainable flushing strategy.

KEYWORDS

PFOS, Perfluorooctane sulfonic acid, Rhamnolipid, Soil flushing, Column testing

This is an open access article published by InterPore under the terms of the Creative Commons Attribution-NonCommercial-NoDerivatives 4.0 International License (CC BY-NC-ND 4.0) (<https://creativecommons.org/licenses/by-nc-nd/4.0/>).



©2025 The Authors

1. INTRODUCTION

Per- and polyfluoroalkyl substances (PFAS) are a group of persistent synthetic chemicals that are associated with detrimental human and ecological health effects and build up in natural environments (12, 19, 29, 60). The release of PFAS from aqueous film forming foam (AFFF) have resulted in some of the most PFAS-contaminated soil and groundwater sites worldwide (26, 36). Conventional in-situ environmental remediation techniques are ineffective in PFAS remediation applications due to the temperature resistance and electrostatic properties of PFAS compounds.

Traditional methods to prevent PFAS in contaminated soils and groundwater from migrating offsite include soil excavation and in-situ soil stabilization (1, 20, 46, 50). Recent studies have explored increasing PFAS desorption from soil and the air-water interface (AWI) with the goal of recovering PFAS-contaminated water from the subsurface for ex-situ treatment. Short-chain PFAS are more soluble and exhibit weaker sorption to air and soil, meaning soil residence times are shorter and retardation during transport is lower than long-chain PFAS (20, 24, 32, 42, 47). At contaminated sites, short-chain PFAS are typically seen at lower concentrations in the unsaturated zone than long-chain PFAS as they leach downwards more rapidly (1, 6, 29, 47). Therefore, long-chain PFAS such as perfluorooctanoic acid (PFOA) and perfluorooctane sulfonic acid (PFOS) are the focus of most PFAS flushing tests, for which laboratory-scale column testing with clean quartz sand is typically used. The type of the functional head group in the PFAS molecule also influences sorption behavior. Kabiri et al. (32) found that PFAS with sulfonated head groups such as PFOS were slower to be flushed from soil than PFAS with carboxylated head groups such as PFOA. The transport of PFAS in the saturated zone is faster than in the vadose zone due to adsorption at the AWI, so higher water content in soil has been suggested to decrease PFAS retardation (2, 7, 16, 24, 27, 38). Altering the pH and ionic strength of the solution has had varied results (32, 38, 39, 47). The presence of some co-contaminants such as chlorinated solvents or co-PFAS can increase retardation of PFAS (4, 18, 35, 62). Higher clay content of soil also can increase PFAS retardation, though higher porosity and therefore higher saturation of clayey soils can decrease PFAS retardation in some cases (1, 37). The transport of PFAS in soils with high organic carbon content is slower than in clean sands due to its affinity for sorption on organic matter (16).

Anionic hydrocarbon surfactants such as sodium dodecylbenzene sulfonate (SDBS) and sodium dodecyl sulfate (SDS), which is found in AFFF, have been suggested to compete with PFAS for adsorption sites at the AWI and on resin (1, 20, 31, 38, 41). The competitive adsorption effect is greater for long-chain PFAS such as PFOS. For short-chain compounds such as perfluorobutanoic acid (PFBA) and perfluorobutane sulfonate (PFBS), the presence of SDS as a co-contaminant actually increases sorption (19). However, short-chain PFAS have low retardation factors of around one, so it is not vital for competitive adsorption effects to take place to aid in soil flushing of short-chain compounds (20). Due to competitive adsorption, flushing PFAS-contaminated soil with a hydrocarbon surfactant could be effective in mobilizing long-chain PFAS adsorbed at the AWI and to soil grains (1, 20, 38, 50).

To date, no PFAS flushing studies have been performed using a commercially available biosurfactant, in place of a hydrocarbon surfactant such as SDS. Biosurfactants are formulated with naturally derived biodegradable compounds from plants or microbes and are therefore a renewable resource (15). Rhamnolipid biosurfactants are anionic surfactants made from the bacteria *Pseudomonas aeruginosa* and have been compared to SDS in efficacy and behavior for remediation applications (15, 17, 40, 45). Identifying an effective biosurfactant is advantageous in that its use would not introduce an additional contaminant to the subsurface as with a hydrocarbon surfactant. Furthermore, no study has been done using a clay- and organic-rich soil, such as the soil commonly found in delta regions where 339 million people live world-wide (14). Use of a relevant representative soil composition is crucial to consider for site remediation applications because soil composition influences PFAS transport behavior.

The objective of this study is to increase PFAS mobility and recoverability in the subsurface by flushing AFFF-contaminated soil with a rhamnolipid biosurfactant. Using column flushing tests, the efficacy of the rhamnolipid solution is compared to that of flushing with water alone. Column tests are designed and optimized to soil collected from an AFFF-contaminated site in The Netherlands. After flushing by tap

water or 0.005% rhamnolipid, eluent samples are analyzed for PFAS concentrations, which are modeled using the advection-dispersion equation considering equilibrium and kinetic adsorption. Retardation factors are estimated for a suite of six PFAS compounds found in AFFF, with a focus on PFOS. Soil-derived phosphate elution is measured for comparison of electrostatic desorption behavior with PFAS desorption.

2. METHODS AND MATERIALS

2.1. Contaminated Site: PFAS Living Lab

Soil samples were collected from the PFAS Living Lab site at Utrecht University, Utrecht, The Netherlands (the Site) in April 2023. The 3000 m² Site was used as a fire safety training facility for Utrecht University until 2014, during which the soil was contaminated with AFFF. Within the Site, an area of 2,100 m² exceeds the Local Maximum Value of 3 µg/kg PFAS in surface soil being the RIVM's^a July 2020 Temporary Action Framework limit (44, 61). In the source zone, the 3 µg/kg PFAS limit is exceeded up to a depth of 1.5 m below ground surface. The soil at the Site is characterized by anthropogenic fill from 0 to 2 m bgs consisting of sand and clay. From 2 to 11 m, Holocene deposits alternate between sandy clay, medium and fine sand, clay and peat. The soil samples were collected in 20 cm intervals from 0 to 100 cm. These samples had an average organic carbon content of 3.4% with 13.3% lutum. The main PFAS contaminant of concern at the Site is PFOS, with soil concentrations up to 95 µg/kg dry weight and in groundwater draining from the site at 1500 ng/L.

Laboratory analysis of soil samples from the April 2023 sampling event was performed by the Vrije Universiteit Amsterdam using their liquid chromatography-mass spectrometry Sciex ExionLC and Sciex 6500+ methodology. The details of the sample clean-up and analysis are provided in Section 1.2 in the **Supplementary Material** (available online) with tabulated measurements in **Supplementary Table S.1**.

2.2. Column Experiments

2.2.1. Column Preparation

Prior to running experiments with PFAS-contaminated soil, the experimental column set-up was tested with clean reference soil, and tests with a non-reactive tracer were performed to identify conservative transport characteristics of the column fill. The methodologies for column packing and tracer tests, as outlined in the following, are based on methods given in *ISO 21268-3* and *US EPA Method 1314* (28, 58).

Soil collected from the Site was mixed with clean sand prior to column packing. Preliminary tests showed that the use of soil from the site alone was not suitable for column testing due to low hydraulic conductivity because of the high clay content in the soil (K_f about $5e - 5$ m/d). We tested different sand/soil ratios with the aim of optimizing the balance between keeping the amount of Site-specific soil high but also maintaining uniform flow within the column and allowing the flushing agent to pass through.

We used virgin 0.161 mm sand sourced from Waternet^b (homogeneity index $I = 1.491$) to mix with the soil. Its hydraulic conductivity was determined by a falling head test with 5m/d and confirmed with calculation of K_f from the particle size distribution, following the procedure of De Rijk et al. (11). The soil collected from the Site was dried at 45°C for 20 hours, ground with a mortar and pestle, and sieved to 2 mm, following the methodology of Nickerson et al. (47), Niarchos et al. (46), and Maizel et al. (42). A low temperature was used to avoid any potential volatilization of PFAS compounds. Mixing of sand and soil occurred manually. Based on the lowest possible pumping rate of 17.5–19 mL/min (technical limitation), we identified 22% soil by weight to be the maximum possible amount. Hydraulic conductivity of the sand/soil mixture was identified as 0.5 m/d, which is two orders of magnitude smaller than the pure sand, but three orders of magnitude larger than the pure soil.

^a Dutch National Institute for Public Health and the Environment

^b <https://www.waternet.nl/en/>

Clear acetate columns (inner diameter 5.5 cm, height 37.5 cm) were dry packed with soil/sand mixture in 2 cm lifts, and tamped 5 times per lift. This consistently resulted in a dry bulk density (ρ_b) of $1.65 \pm 0.01 \text{ g/cm}^3$ each time the column was packed. Steel mesh screens (325 mesh, $42 \mu\text{m}$ pore diameter) were included at the bottom and top of the column to disperse flow and ensure the inlet and outlet did not clog (10, 24, 38). Up-flow experiment design was used to simulate fully saturated conditions (28, 42, 58, 64). This methodology ensures that bubbles are not trapped in the column during saturation. An equilibration period of approximately 24 hours followed column packing for each experiment (43, 46, 58, 64). Each flushing treatment was performed once.

The materials used in the experimental setup did not include those that are known to contain or interact strongly with PFAS (e.g., teflon, low-density polyethylene, glass) (30). We decided to use acetate columns, as they have been shown to be among the best materials for PFAS testing (along with PVC) (22, 46). A method blank was performed with 100% clean sand in which tap water was pumped through the column. The test was performed after a test with PFAS-contaminated soil. None of the tested PFAS compounds were detected in the effluent, confirming that the acetate column does not affect PFAS concentrations in effluent.

2.2.2. Non-reactive Tracer Test

We performed conservative tracer tests in all columns to identify flow and conservative transport characteristics. A preliminary tracer test was performed on an uncontaminated soil sample, following column packing and equilibration. We performed the same type of tracer tests in the columns with contaminated soil after the PFAS flushing experiments. In this way, we were able to calculate soil parameters and confirm consistency of column packing without distorting PFAS concentrations.

Breakthrough curves (BTCs) of 0.01 molar NaBr nonreactive tracer were fitted to solutions of the one-dimensional advection-dispersion equation (Eq. 1):

$$\frac{\partial C}{\partial t} = -v \frac{\partial C}{\partial x} + D \frac{\partial^2 C}{\partial x^2} \quad (1)$$

where $C(x, t)$ is the concentration of the solute in space x (position along the column) and time t is normalized by the background naturally occurring salt concentration, v is pore velocity. $D = \alpha_L \cdot v + D_{\text{diff}}$ is the hydrodynamic dispersion coefficient, being the sum of dispersion (α_L is the longitudinal dispersivity) and diffusion D_{diff} . At the time and space scale of the experiment, the effect of diffusion is small and can therefore be neglected.

For data fitting and parameter identification we used the CXTFIT program of STANMOD^c (STudio of ANalytical MODels) (52, 55) which provides (semi-) analytical solutions of Equation 1 for a variety of initial and boundary conditions, including those reflecting the experimental conditions. The CXTFIT program uses a nonlinear least-squares method for parameter optimization.

Soil characteristics identified from the reference tracer test are longitudinal dispersivity $\alpha_L = 0.674 \text{ cm}$; porosity $\theta = 0.44$; and bulk density of $\rho_b = 1.65 \text{ g/cm}^3$. Breakthrough curve results of the reference tracer test are visualized in **Supplementary Figure S3** (**Supplementary Material** available online) and those of the tracer tests performed after PFAS flushing in **Supplementary Figure S4** (**Supplementary Material** available online). For the latter, identified parameters of porosity θ and bulk density ρ_b were consistent with those of the reference tracer test.

2.2.3. PFAS Flushing Experiments

We performed PFAS flushing tests with tap water and 0.005% rhamnolipid solution, respectively. The PFAS-contaminated soil sample **B-3 0.20–0.40 m** was used in the tap water test, and sample **B-3 0.60–0.80 m** was used in the rhamnolipid test. These samples were selected because their reference samples (B-2 for the same depths, see **Supplementary Table S1** for details; available online) have the same total PFOS concentrations ($69 \mu\text{g/kg}$). The soil characteristics of these samples were similar, both being a light clay with 12–17.5% lutum with 3–4% organic carbon. Columns were prepared as outlined in Section 2.2

^c <https://www.pc-progress.com/en/Default.aspx?stanmod>

in the [Supplementary Material](#) (available online). The entirety of each soil sample was used such that soil/sand mixtures contained 20% and 21% soil each, which is below the 22% possible soil content threshold. This resulted in a porosity of 44% and 43%, respectively.

For the rhamnolipid flushing test, a 0.005% rhamnolipid in tap water solution was created with a 90% purity rhamnolipid mixture of di-rhamnolipid and mono-rhamnolipid^d. This solution composition was first tested with a column containing 22% reference soil to confirm that no bubbles or foam were created that could alter flow characteristics. Rhamnolipid was selected following a review of biosurfactants because it meets the following criteria: **(i)** it behaves much like a previously tested hydrocarbon surfactant; **(ii)** it is already widely manufactured; and **(iii)** it is cost-effective in comparison to other biosurfactants. Rhamnolipid effectively reduces interfacial tension values to levels comparable to common hydrocarbon surfactants, such as SDS (40) and has been shown to aid in flushing contaminants from soils (15, 17, 45). We chose a concentration of 0.005% (or 0.05 g/L) as this is approximately the median of the range (0.005–0.9 g/L) of the critical micelle concentration of rhamnolipid (17, 23, 34, 40, 45, 48, 54).

The flushing test started with 24 hours of equilibration with tap water for the water test and rhamnolipid solution for the rhamnolipid test. Then, the columns were flushed with approximately 24 pore volumes (PV) each at a flow rate of 19 mL/min. Flow velocities v were in the range of 1.71–1.82 cm/min and hydraulic retention time (equivalent to one pore volume) was in the range of 20.6–21.9 min. Twenty-four water eluate samples of 400 mL each were collected in 500 mL polypropylene bottles and frozen at -20°C to stabilize the samples until analysis (63). Even-numbered eluate samples were used for phosphate analysis and odd-numbered samples were used for PFAS analysis. Following the flushing tests, the non-reactive tracer test was completed to confirm consistency of column packing and provide data for soil parameter calculations.

2.2.4. Aqueous PFAS Analysis

Laboratory analysis of the odd-numbered aqueous PFAS eluate samples (1 to 23) was performed in facilities at the Utrecht University Veterinary School. Six common types of PFAS found at the site were analyzed by a methodology based on EPA *Method 1633* for PFAS analysis by liquid chromatography-mass spectrometry (LC-MS): PFBA, perfluorohexanoic acid (PFHxA), PFOA, PFBS, perfluorohexane sulphonic acid (PFHxS), and PFOS (57). The PFAS extraction was performed using weak ion exchange sorbent cartridges. Analysis was performed using coupled high-performance liquid chromatography-mass spectrometry^e. All laboratory QA/QC checks were passed. Detailed information on analysis methodology and quality control is provided in Section 1.3 of the [Supplementary Material](#) (available online). Tabulated measured concentrations for all PFAS compounds are summarized in **Tables S2** and **S3** in the [Supplementary Material](#) (available online).

2.2.5. Phosphate Analysis

Phosphorus can be an indicator of water movement and soil conditions in soil profiles and therefore was included to determine if a correlation between PO_4 and PFAS desorption from soil could be observed (53). Phosphate is a negatively charged oxyanion known to have strong (electrostatic) interactions with positive charged soil constituents like Fe-hydroxides. Anionic PFAS may be subject to the same kind of interactions.

Even-numbered eluate samples (2 to 24) from both the water flushing experiment and the rhamnolipid flushing experiment were analyzed for phosphate. Each of the 24 samples were acidified with HCl (9.9 mL sample per 0.1 mL 35% HCl). One blank was also analyzed with 0.1M HCl in ultra-pure water. Samples were analyzed spectrophotometrically using a Gallery Discrete Analyzer^f at wavelength 880 nm. The

^d Sigma-Aldrich (Merck): <https://www.sigmaaldrich.com/NL/en/product/sigma/r90>

^e Shimadzu Nexera XR and Shimadzu LCMS-8050: <https://www.shimadzu.nl/products/liquid-chromatography/hplcu/hplc/nexera-series/index.html> & <https://www.shimadzu.nl/products/liquid-chromatography-mass-spectrometry/triple-quadrupole-lc-msms/lcms-8050/index.html>

^f Thermo Scientific: <https://www.thermofisher.com/nl/en/home/industrial/chromatography/automated-wet->

Phosphate Low setting was used with a 1000 $\mu\text{g/L}$ standard for P calibration. Once every seven samples, the sample was reanalyzed to confirm precision of the machine. These values were all within an acceptable range ($\leq 0.6\%$ deviation). Tabulated measured phosphate concentrations are summarized in **Supplementary Table S4** in the **Supplementary Material** (Available online).

2.2.6. Batch Testing

Supplementary batch testing was performed to confirm the results of the column tests. The removal of PFAS from contaminated soil was measured in tap water and in a 0.005% rhamnolipid solution, each used to wash separate batches of soil. More details on the batch testing methodology and results are provided in Section 1.5 of the **Supplementary Material** (available online).

2.3. PFAS Concentration Analysis

2.3.1. Mass Balance

The mass balance for each flushing test was calculated to determine what percentage of the total initial mass of PFAS in the column was flushed over 24 PVs using **Equation 2**:

$$\%_{\text{PFAS eluted}} = \frac{m_w^{\text{PFAS}}}{m_s^{\text{PFAS}}} \cdot 100\% = \frac{\sum_{i=0}^{24} [C_i^{\text{PFAS}} \cdot V_w]}{W_s^{\text{PFAS}} \cdot m_s} \cdot 100\% \quad (2)$$

where the total mass of PFAS in the eluent m_w^{PFAS} results from the sum of all dissolved eluate concentrations of the PFAS compound C_i^{PFAS} [ng/L] and the volume of one eluate sample V_w [L] (approximately equal to PV). The initial mass of PFAS in the column sample m_s^{PFAS} was calculated from the initial mass fraction of the PFAS W_s^{PFAS} [ng/kg] in the duplicate of the soil sample used for the respective column test, and the mass of contaminated soil m_s [kg] in the column. Linear interpolation was used to estimate the concentrations of even-numbered samples that were used for phosphate analysis.

2.3.2. Transport Modeling

Given the complexity of PFAS adsorption, we chose to analyze PFAS eluate concentrations with a reactive transport model including two reactive adsorption terms, a fast (equilibrium) and a slow (kinetic) one (21). Particularly, the slowly decreasing PFOS concentration indicated the need for a slow (kinetic) adsorption mechanism.

We formulate the advection-dispersion equation with linear equilibrium adsorption accounting for fast-reacting adsorption sites and first-order kinetic adsorption following the dimensionless formulation of Toride, et al. (55; Eq. 3):

$$\begin{aligned} \beta R \frac{\partial C}{\partial T} &= -\frac{\partial C}{\partial X} + \frac{1}{P} \frac{\partial^2 C}{\partial X^2} - \omega(C - C_s) \\ (1 - \beta)R \frac{\partial C_s}{\partial T} &= \omega(C - C_s) \end{aligned} \quad (3)$$

where $C = C^{\text{PFAS}}/C_0^{\text{PFAS}}$ is the normalized concentration of the PFAS compound in solution and C_s is the normalized concentration of PFAS adsorbed kinetically. $T = v \cdot t/L$ and $X = x/L$ are dimensionless time and distance, respectively, with average flow velocity v and length of the column L . $P = \frac{v \cdot L}{D}$ is the pecllet number, where D is again the dispersion coefficient. $R = 1 + \rho_b \cdot K_d/\theta$ is the retardation factor with K_d [mL/g] being the linear adsorption coefficient, ρ_b [g/mL] being the bulk density and θ being the porosity. β is the dimensionless partitioning coefficient and ω is the dimensionless mass transfer coefficient defined as **Equation 4**:

$$\beta = \frac{\theta + f \rho_b K_d}{\theta + \rho_b K_d} \quad \omega = \frac{\lambda(1 - \beta)RL}{v} \quad (4)$$

where f [-] is the fraction of the exchange sites that are at equilibrium, and λ [1/min] is the first-order kinetic adsorption rate coefficient (sometimes also called α , but we renamed it to avoid confusion with dispersivity α_L). Note the similarity of Equation 3 to the dual porosity model, which has the same mathematical formulation but does not reflect the physical meaning of the processes modelled here.

We again made use of STANMOD/CXTFIT (52, 55) to fit PFAS eluate concentrations and identify adsorption parameters R , β and ω for those quantities that showed significant retention. Conservative transport parameters remained fixed (using velocity v and dispersion D identified in the tracer tests) during the fit of PFAS adsorption properties. Specifics on model settings and technical details such as boundary conditions and the fitting process are outlined in Section 2.1 in the [Supplementary Material](#) (available online).

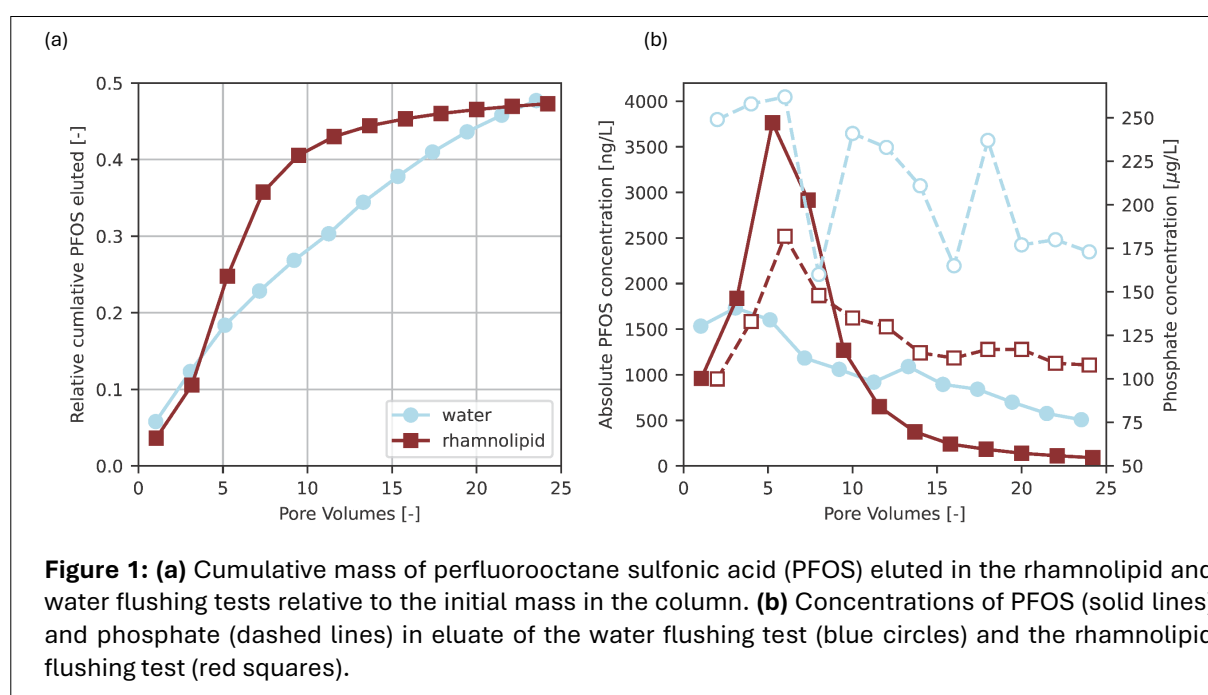
3. RESULTS AND DISCUSSION

3.1. PFOS Flushing

We primarily focus on the results of PFOS in our flushing tests. The PFOS concentrations in soil at AFFF-impacted sites are the highest of all PFAS compounds, and they are suggested to have the strongest sorption to soil (32, 61). The total percent mass of PFOS flushed for each test was about the same at 48% for the water test and 46% for the rhamnolipid test. However, during the first half of each test (12 PV), only 64% of the total 9909 ng PFOS for the water flushing test was eluted, while 91% of the total 9852 ng of PFOS in the rhamnolipid flushing test was eluted. The faster rate of PFOS elution in the rhamnolipid test can be seen in the steep slope of the cumulative mass eluted (Fig. 1a). This indicates that flushing with the rhamnolipid solution was more efficient in removing PFOS than with water alone.

Figure 1b shows that rhamnolipid flushing resulted in much higher PFOS concentrations within the first 10 pore volumes. While water alone flushed out the PFOS more steadily, with the highest concentration of PFOS (1734 ng/L) occurring at three PVs, the peak concentration of PFOS (3764 ng/L) in the rhamnolipid flushing test occurred a little later (at five PVs) but was more than twice the peak of the water flushing test. The peak in PFOS eluate concentration aligns with the peak in phosphate eluate concentration in the rhamnolipid test at 5 to 6 PV.

We attribute the faster flushing of PFOS observed in the rhamnolipid experiments to changes in zeta potential and competitive electrostatic adsorption, which have also been identified as possible drivers of enhanced PFAS elution with other surfactants. Because most PFAS are negatively charged, they tend



to sorb more strongly to positively charged soils, with soil acidity influencing this interaction. Anionic surfactants produce negative zeta potentials which potentially desorb the PFAS from the soil particles. Dissolved PFOS then competes with rhamnolipid for adsorption sites. This effect is independent of equilibration time, as the total amount of PFAS and rhamnolipid molecules in solution compete for adsorption sites on the soil surface. The dynamic sorption and desorption processes of both PFAS and the rhamnolipid result in overall higher concentrations of PFAS in solution than in the scenario without rhamnolipid present.

Following the peak in PFOS elution, the amount of PFOS flushed per PV in the second half of the rhamnolipid test dropped quickly. The efficacy of the rhamnolipid may decrease when the PFOS concentration drops below a threshold, as the competitive adsorption effects no longer exist to the extent they do when PFOS concentration is high. It would therefore be important to test different concentrations of both PFOS and rhamnolipid to see what the best combination is and better define thresholds for effective competitive adsorption. For example, increasing the concentration of rhamnolipid could potentially leach PFOS to a lower residual adsorbed concentration.

The concentrations of phosphate in eluate from the water flushing test was higher overall than the rhamnolipid flushing test (**Fig. 1b**). The calculated total mass of phosphate eluted by linear interpolation between measurements was a factor of 1.7 higher for the water flushing test than the rhamnolipid flushing test, at 2.02 mg and 1.21 mg, respectively. Since initial PO_4 soil content was not measured, this difference in total phosphate eluted does not have a clear explanation.

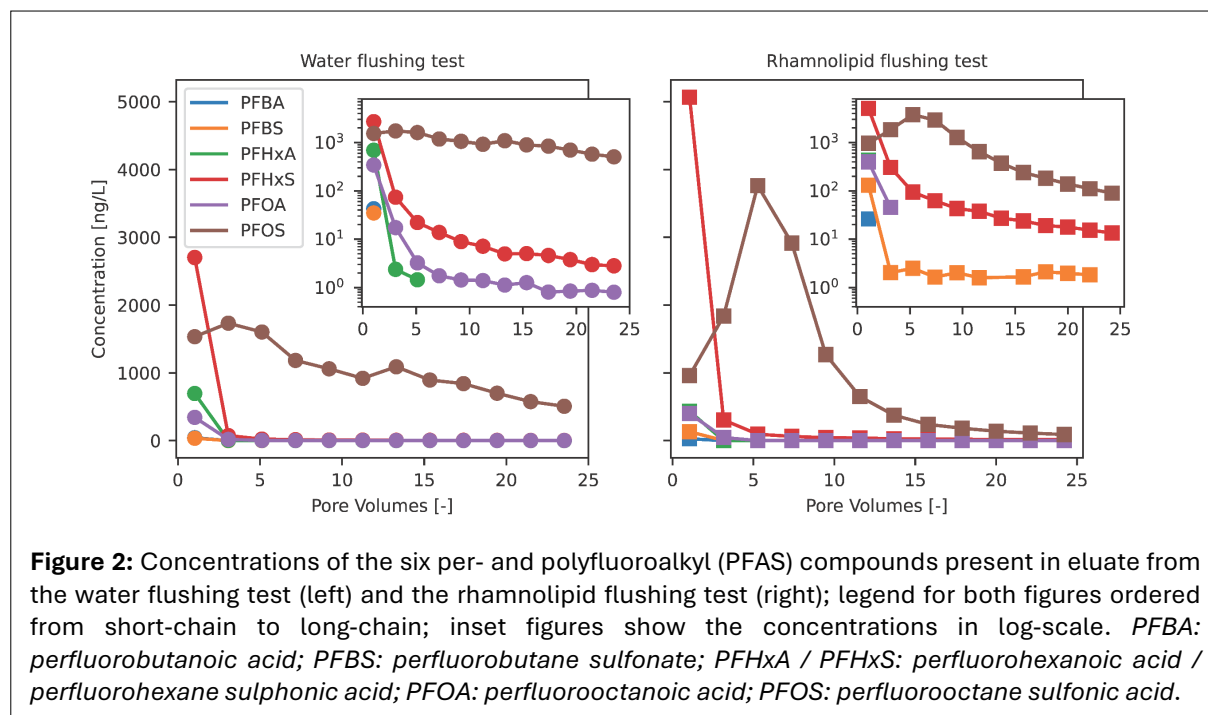
The delayed peak in PFOS elution in the rhamnolipid test echoes the PO_4 elution curve (**Fig. 1**). Because the column was allowed to equilibrate with the rhamnolipid solution for 24 hours prior to flushing, it is not likely a result of a delayed equilibrium with the solution occurring only after about 5 PVs. The drying and grinding of soil with a mortar and pestle resulted in a dual porosity domain, in which there are clay grain clusters that are less than 2 mm in diameter mixed with individual soil and sand grains. The PFOS within the clusters of clay may be more strongly adsorbed to those clay grains due to hydrophobic nature of clay minerals, and take longer to be flushed out (36). There are also possible effects from the two-site adsorption, with one equilibrium site having fast exchange and the other having slow, non-equilibrium exchange with solution. Therefore, PFOS adsorbed at the slow exchange site will take longer to be flushed out. In both the water flushing and rhamnolipid flushing tests, these effects result in slower PFOS elution overall, consistent with results noted previously.

The alignment of PO_4 eluate concentrations with the PFOS eluate concentration also supports the idea that competitive adsorption, specifically electrostatic adsorption, is a factor (**Fig. 1b**). Negatively charged PO_4 adsorption/desorption behavior is driven by the electrostatic potential between the soil and the PO_4 (3, 33). If the negatively charged rhamnolipid is competitively adsorbing to soil and resulting in electrostatic desorption of PO_4 , the similar elution pattern indicates that competitive electrostatic desorption drives PFOS desorption as well. The pattern of other PFAS compound elution does not match the PO_4 elution pattern because they have weaker adsorption to soil and flush out quickly. Moreover, electrostatic adsorption behavior may vary between PFAS compound types (37). Since PFOS is the dominant PFAS type present in AFFF, understanding the competitive electrostatic adsorption effect induced by rhamnolipid is critical.

3.2. Flushing of other PFAS Compounds

3.2.1. Eluate concentrations

Eluate concentrations of all six PFAS compounds are displayed for both the water and rhamnolipid flushing tests in **Figure 2**. The PFAS elution curves for both tests display transport characteristics expected based on chain length and resulting sorption behavior. Elution of short-chain PFAS compounds PFBA, PFBS, PFHxA and PFHxS is fast compared to PFOS, with maximum eluate concentrations in the first PV. This is consistent with the literature, in which PFOS is the slowest to be removed (2, 20, 24, 35, 42, 46, 47).

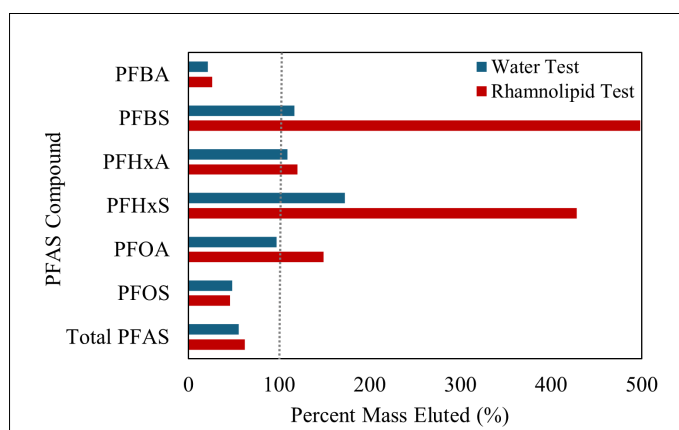


Elution curves for PFHxS show a large peak at the first PV (**Fig. 2**). In fact, the highest concentration of any PFAS in eluate measured was PFHxS in the first PV for both the water and rhamnolipid flushing tests at 2702.7 ng/L and 5067.3 ng/L, respectively. Though PFHxS concentrations did not reach zero by the end of 24 PVs, fast elution is evidenced by the high concentration peak in the first PV and contrasting low concentrations by PV 24 at 2.8 ng/L and 13.4 ng/L.

3.2.2. Mass Balance

Mass balance calculations for PFHxA and PFOA in both the water and rhamnolipid flushing tests, as well as for PFBS in the water flushing test, showed approximately 100% recovery, indicating that nearly all of these compounds were flushed out of the columns (**Fig. 3**). This means that the concentrations eluted in the final pore volume(s) were below the method detection limits (0.0004 ng/L, 0.003 ng/L, and 0.0003 ng/L, respectively, for the water flushing test, and 0.006 ng/L and 0.015 ng/L, respectively, for the rhamnolipid flushing test), as no measurable amounts of these compounds remained in the columns by the end of the tests (**Fig. 2**). Perfluorobutane sulfonate also shows a pattern typical of short-chain PFAS with the highest concentration in the first PV and concentrations below method detection limits by the end of each test.

Mass balance calculations exemplify the varying flushing behavior between short-chain PFAS compounds PFBA, PFBS, PFHxA and PFHxS and long-chain PFOA. Because PFBA eluate concentrations were below the method detection limit after one PV, it would seem that all PFBA was removed from the columns. However, the mass balance for both tests was below 100% at 22% and 26%, respectively (**Fig. 3**). Since PFBA is a short-chain PFAS, it is more water-soluble and would be present dominantly in the dissolved phase in a water-saturated soil sample (8). It is likely



that the soil samples analyzed had a higher water content than the corresponding samples actually used for the column tests, resulting in an overestimation of the initial mass of PFBA in the column. It has also been suggested that PFBA is volatile and may have been lost during the drying of the soil (59). However, as the duplicate soil sample was dried prior to PFAS analysis in April 2023 using the same method as the column test sample, this effect is unlikely to have contributed to the observed mass balance discrepancy.

Both PFBS and PFHxS had extremely high recoveries in eluate, especially during the rhamnolipid flushing test. The mass of PFBS eluted from the column in the rhamnolipid test was 4.98 times the PFBS concentration determined in the reference soil sample. Similarly, PFHxS concentrations in the eluted compared to those in the reference soil sample were 4.25 times as much for the rhamnolipid test and 1.73 for the water flushing test. Because laboratory QA/QC passed all checks for these compounds, a lab error is not a likely explanation. A possible contributor to the high recovery is a relative heterogeneous distribution of PFBS and PFHxS compared to other PFAS compounds in the subsurface. The concentrations of PFBS in other sampling intervals of the same sampling location (above and below the sample used for the rhamnolipid test at 60–80 cm) was 3.3 times higher (values listed in **Supplementary Table S1**, available online in the **Supplementary Material**). Similarly, the PFHxS concentrations above and below the sample interval were 2.4 and 3 times higher than the sample, respectively. If errors were made in sample collection, or if samples were not properly homogenized, it is possible that the sample we used in the column had higher initial concentrations of PFBS and PFHxS than we assumed.

However, this difference could only account for a percent mass elution of at most 150% to 175%, not the 428% to 499% observed. The remaining difference in mass eluted versus initial mass in the soil may be explained with PFAS precursors. Aqueous film-forming foam contains precursors to sulfonated PFAS. When the AFFF-contaminated soil was oxidized in preparation of the columns, the precursors could have been converted to PFBS and PFHxS, which are both sulfonated PFAS (25, 51, 56). An AFFF study showed that precursors accounted for 23% to 28% of the total concentration of PFAS in soil (25). Following oxidation in groundwater, PFHxS was produced, as seen in much higher PFHxS:PFOS ratios than in soil. Though precursors were not measured in our soil, they are likely present due to the AFFF origin of the PFAS (9, 25, 42). Whether precursor conversion to PFBS and PFHxS can account for nearly 500% recovery depends on the initial mass of precursors present in the AFFF formulation, which would need to be known to confirm this effect.

3.3. PFAS Desorption Modeling

Eluate concentrations of PFAS for both flushing tests have been fitted to the transport model (Eq. 3) to quantify the equilibrium and kinetic adsorption characteristics. Parameters f , K_d and λ were calculated using Equation 4 from the fitted R , β and ω values. Identified parameters are summarized in **Table 1**. Visualizations of the fits are provided in **Supplementary Figures S5** and **S6** (available online in the **Supplementary Material**). We reasoned earlier that differences in the flushing results are the results of competitive adsorption between PFAS and surfactant. While the physics of the process at pore scale are

Table 1: Adsorption parameters for flushing tests showing behavior of two-site kinetic adsorption: retardation factor R quantifying fast equilibrium adsorption, K_d [mL/g] is the linear adsorption coefficient, f [-] is the fraction of the exchange sites that are at equilibrium, and λ [1/min] is the first-order kinetic adsorption rate coefficient.

Compound	Flushing test	R [-]	K_d [mL/g]	f [-]	λ [1/min]
PFOS	Water	22.3	5.24	0.17	0.004
PFOS	Rhamnolipid	9.76	1.56	0.25	0.013
PFHxS	Water	2.07	0.23	0.88	0.022
PFHxS	Rhamnolipid	2.47	0.38	0.87	0.007
PFOA	Water	2.18	0.24	0.81	0.038
PFBS	Rhamnolipid	2.45	0.38	0.59	0.001

PFOS: perfluorooctane sulfonic acid; PFHxS: perfluorohexane sulphonic acid; PFOA: perfluorooctanoic acid; PFBS: perfluorobutane sulfonate

not part of the transport model, its effects are captured - and even quantified - in the different adsorption characteristics and parameters, such as the retardation factor R .

3.3.1. PFOS Desorption

Fitted retardation factors for PFOS were significantly lower in the rhamnolipid flushing test ($R_r = 9.76$) than in the water flushing test ($R_w = 22.3 \pm 0.9$). This means that transport of PFOS was less retarded due to soil adsorption when rhamnolipid was used to flush the soil than when water was used. Consequently, values of the linear adsorption coefficients K_d of the fast sites for PFOS are higher for the water test than for the rhamnolipid test. Both values are significantly higher than for the other short chain and PFOA compounds (Table 1). However, as K_d values can be difficult to estimate, the experiment should be repeated to confirm these results (16).

Modeling results also indicate that rhamnolipid mobilizes more PFAS from slow sites than water alone. The portion of sites that are fast (f) versus slow (55) is lower in the water flushing test ($f_w = 0.17$) than in the rhamnolipid flushing test ($f_r = 0.25$). At the same time, the low values of f indicate that there are more slow exchange sites than fast equilibrium sites in both cases, thus confirming the strong retardation of PFOS in soil. Furthermore, the f values for PFOS are lower than those of the other PFAS compounds (Table 1). This result is consistent with expectations, as PFOS exhibits stronger non-equilibrium adsorption to soil compared to short-chain PFAS compounds, which display nearly linear sorption behavior (4).

3.3.2. Other PFAS Compounds Desorption

All PFAS, except PFOS, exhibited rapid decreases in concentration during the flushing experiments (Fig. 2b). For several quantities, such as PFBA and PFHxA, the second sampling point (3 PVs) already showed no concentrations above the detection limit. In these cases, we concluded that desorption is fast and kinetic sorption effects are negligible. This aligns with other results (4, 20, 46) indicating that short-chain PFAS such as PFBA, PFBS and PFHxA often approach linear equilibrium adsorption behavior, especially at low concentrations.

For all short-chain PFAS, retardation factors close to a value of 1 are expected. Given the missing sampling points between 1 PV and 3 PV, we can only conclude that the linear retardation coefficient R is ≤ 3 for PFHxA and PFBA in both tests, as well as for PFBS in the water test and PFOA in the rhamnolipid test. For those PFAS that exhibited non-zero concentrations throughout the entire test (PFHxS for both tests, PFOA for the water, and PFBS for the rhamnolipid test), the retardation factors of approximately $R = 2$ determined by the two-site adsorption model confirm the rapid equilibrium desorption (Table 1).

Per- and polyfluoroalkyl compounds other than PFOS show similar desorption behavior with water and with a rhamnolipid biosurfactant. This is because the short-chained PFAS compounds PFBA, PFBS, PFHxA, PFHxS, and long-chained PFOA are not retarded as much as PFOS overall (2, 20, 24, 35, 42). The calculated fraction of sites at equilibrium f also verify this result with f values between 0.59 and 0.88 being much higher than those for PFOS (Table 1). With a higher fraction of equilibrium adsorption sites, the short-chain PFAS will desorb more quickly from soil than PFAS with a low fraction of equilibrium adsorption sites. This confirms the expected result that short-chain PFAS will have greater mobility and be less retarded in the subsurface.

3.3.3. Comparison to other Studies

Our retardation values (R) for saturated PFOS transport ($R_w = 22.3$ and $R_r = 9.76$) are higher overall than reported in other column studies. In fact, these values fall within the range of $R = 2.10$ – 18.47 for unsaturated conditions in previous studies (2, 5, 6, 7, 31, 38, 39). The same applies for the retardation factors (R) of PFOA. While values reported in literature for saturated PFOA transport range from $R = 1.06$ – 1.68 , our results of ($R \approx 2$) are more consistent with those observed under unsaturated conditions ($R = 1.2$ – 3.18) (2, 4, 5, 7, 31, 38, 39, 62). This may be because our experiment used soil from the environment rather than clean quartz sand. Retardation of PFOS in the field is calculated to be much higher ($R = 16$ – 1355) (21, 24). The soil used here has a high organic carbon content of 3.4% compared to other surface soils or the Accusand typically used in column tests. Per- and polyfluoroalkyl compounds

tend to adsorb to the organic fraction of soil (13, 16, 29, 31, 46, 49). Additionally, the high clay content of our soil may result in slower desorption (1). Negatively charged clay particles in soil tend to increase PFAS adsorption, especially for long-chained PFAS compounds such as PFOS (37).

Our results are well in line with other studies on the effect of (traditional) surfactants on PFAS flushing. The R -values of PFOS obtained from rhamnolipid and water flushing ($R_w = 22.3$ compared to $R_r = 9.76$) show similar patterns to the calculated R -values from batch testing reported by Guelfo and Higgins (18), where PFOS R -values are substantially lower in the presence of the hydrocarbon surfactant SDS ($R = 9.08$ compared to $R = 18.47$). Guelfo and Higgins (18) reported that R -values for the other PFAS compounds remain largely the same or even increase with the addition of SDS as we also see with rhamnolipid in our study. Ji et al. (31) also saw a slight increase in retardation with SDS for PFOA in both saturated and unsaturated conditions. Encouragingly, the similarities between PFOS and PFOA R -values using a hydrocarbon surfactant SDS and a rhamnolipid biosurfactant supports our hypothesis that rhamnolipid behaves much like traditional anionic surfactants in terms of reducing retardation of PFAS in the subsurface.

4. SUMMARY AND CONCLUSION

This study is the first to both explore the feasibility of using a biosurfactant to mobilize PFAS in saturated soil and to use a soil characteristic of delta areas to perform PFAS transport experiments. The flushing of PFOS with the biosurfactant rhamnolipid was more efficient than with water alone; 91% of PFOS mass was eluted by the rhamnolipid solution in the first 12 pore volumes, with water taking twice as much time. Similarities between phosphate and PFOS desorption behavior indicate that competitive electrostatic adsorption by the rhamnolipid biosurfactant may be acting to increase desorption of PFOS and speed up removal from soil. Modeled retardation values for PFOS confirm this result; R -values are 2.3 times lower when the column is flushed by the rhamnolipid solution than by water.

Analysis of PFOS breakthrough curves exhibit the need to account for different adsorption sites, including a fast (equilibrium) and a slow (kinetic) adsorption mechanism. We link the fast adsorption, quantified by the retardation factor (R) to electrostatic desorption accelerated by anionic surfactants producing negative zeta potentials. The mechanisms of the slow adsorption process require more in depth study of the physical situation. It is potentially the result of rate-limited desorption from the contaminated clayish soil which was mixed with sand for the column tests.

For several short chain PFAS, we measured concentrations that significantly exceeded the expected determined from duplicate soil samples. We attribute this primarily to precursor transformation, which is a known effect for AFFF contaminated soil. For future studies, we recommend PFAS concentration measurements at different times to track precursor transformation for PFAS components PFBS and PFHxS.

While it is well known that PFAS sorb to the air-water interface in unsaturated soils, our study confirmed that transport of PFOS is also strongly impacted by sorption in saturated porous media. In contrast, short chain PFAS and PFOA are only moderately retarded. However, we expect other PFAS—specifically linear sulfonated PFAS with carbon chain lengths longer than C8—to exhibit behavior to that of PFOS.

Among the various sorption mechanisms, the electrostatic (de-)sorption of PFAS in soils remains poorly understood. Because PFAS are predominantly negatively charged, they are expected to sorb more strongly to positively charged soils, where soil acidity plays a role. We use anionic surfactants to produce negative zeta potentials and thereby promote PFAS desorption from soil particles in our proof-of-principle tests, which primarily employed clays. Future research should include testing this method on sandy soils, which are usually more acidic and therefore more positively charged, which makes it potentially harder to influence the desorption mechanism.

While our column study is useful to identify hydrogeochemical parameters and physico-chemical processes involved, it does not reflect field conditions. Injection rates were high, putting constraints to the applicable soil regarding hydraulic conductivity. Redesigning the columns to perform long-term

flushing in low conductivity soils is an option to test applicability of biosurfactants. However, we doubt that field-scale soil flushing will be a feasible strategy for low hydraulic conductivity clay-rich soils. In this line, we conclude that flushing is a potential strategy for permeable (sandy) soils with hydraulic conductivities of at least 1m/d. However, applicability to sandy soils must be tested given their difference in charge compared to clays.

Our column tests show promising first results for developing biosurfactant flushing methods for sustainable PFOS remediation. Implications of our work for soil-water practitioners lie in potential remediation strategy design, also for unsaturated soil, e.g. considering soil saturation as part of the operation. Flushing PFOS from soil is feasible when the soil is saturated with a biodegradable surfactant, making this a promising strategy for optimization. Follow-up work is needed to test varying concentrations of PFAS, investigate optimal concentrations of bio-surfactant, test different flow velocities in different soil types, and test flushing in unsaturated PFAS-contaminated soil. This can eventually confirm the viability of a rhamnolipid biosurfactant for use in a flushing remediation strategy for AFFF-contaminated sites.

STATEMENTS AND DECLARATIONS

Supplementary Material

The following material is available [online](#) as a single pdf available: Laboratory reports and figures from the April 2023 soil sampling event; Batch testing methodology and summary of results; PFAS laboratory analysis methodology details and quality assurance/quality control; Fitted breakthrough curves in CXTFIT of preliminary tracer tests and water/rhamnolipid flushing tests; Log-scale PFAS elution curve figures for both water and rhamnolipid flushing tests; CXTFIT input parameters used for the fitting model; Complete PFAS and phosphorous eluate concentration results from the water and rhamnolipid flushing tests; Fitted PFAS elution curves from one-dimensional CXTFIT model; Log-scale fitted PFAS elution curves from one-dimensional CXTFIT model; Hydrogeological parameters calculated from one-dimensional model fitting results.

Acknowledgements

The authors thank the Utrecht University Center for Living Labs, especially the Living Lab: PFAS Remediation research group for their contributions and support for this project.

Author Contributions

Sophie Hibben: data curation, formal analysis, investigation, methodology, project administration, software, validation, visualization, writing - original draft, writing - review & editing. **Alraune Zech:** conceptualization, project administration, resources, software, supervision, validation, writing - review & editing. **Bas von der Grift:** methodology, writing - review & editing. **Jacco Koekoek:** formal analysis, investigation. **Sicco Brandsma:** formal analysis, investigation. **Johan van Leeuwen:** conceptualization, funding acquisition, resources, supervision, writing - review & editing.

Conflicts of Interest

There are no conflicts of interest to declare.

Data, Code & Protocol Availability

Data and protocols are available in the [Supplementary Material](#).

Funding Received

The authors received financial support from Utrecht University through the *Living Lab: PFAS Remediation*.

ORCID IDs

Sophie R. Hibben	 https://orcid.org/0009-0006-7893-7655
Alraune Zech	 https://orcid.org/0000-0002-8783-6198
Bas van der Grift	 https://orcid.org/0000-0003-4069-6703
Jacco Koekoek	 https://orcid.org/0000-0002-5231-084X
Sicco Brandsma	 https://orcid.org/0000-0003-4188-4730
Johan van Leeuwen	 https://orcid.org/0000-0002-1925-1550

REFERENCES

1. Abou-Khalil, C., Sarkar, D., Braykaa, P., & Boufadel, M. C. (2022). Mobilization of per- and polyfluoroalkyl substances (PFAS) in soils: A review. *Current Pollution Reports*, 8(4), 422–444. <https://doi.org/10.1007/s40726-022-00241-8>
2. Abraham, J. E. F., Mumford, K. G., Patch, D. J., & Weber, K. P. (2022). Retention of PFOS and PFOA mixtures by trapped gas bubbles in porous media. *Environmental Science & Technology*, 56(22), 15489–15498. <https://doi.org/10.1021/acs.est.2c00882>
3. Barrow, N. J. (2015). A mechanistic model for describing the sorption and desorption of phosphate by soil. *European Journal of Soil Science*, 66(1), 9–18. https://doi.org/10.1111/ejss.12198_2
4. Brusseau, M. L. (2020). Simulating PFAS transport influenced by rate-limited multi-process retention. *Water Research*, 168, 115179. <https://doi.org/10.1016/j.watres.2019.115179>
5. Brusseau, M. L., Guo, B., Huang, D., Yan, N., & Lyu, Y. (2021). Ideal versus nonideal transport of PFAS in unsaturated porous media. *Water Research*, 202, 117405. <https://doi.org/10.1016/j.watres.2021.117405>
6. Brusseau, M. L., Lyu, Y., Yan, N., & Guo, B. (2020). Low-concentration tracer tests to measure air-water interfacial area in porous media. *Chemosphere*, 250, 126305. <https://doi.org/10.1016/j.chemosphere.2020.126305>
7. Brusseau, M. L., Yan, N., Van Glubt, S., Wang, Y., Chen, W., et al. (2019). Comprehensive retention model for PFAS transport in subsurface systems. *Water Research*, 148, 41–50. <https://doi.org/10.1016/j.watres.2018.10.035>
8. Chen, H., Reinhard, M., Nguyen, T. V., You, L., He, Y., & Gin, K. Y.-H. (2017). Characterization of occurrence, sources and sinks of perfluoroalkyl and polyfluoroalkyl substances (PFASs) in a tropical urban catchment. *Environmental Pollution*, 227, 397–405. <https://doi.org/10.1016/j.envpol.2017.04.091>
9. D'Agostino, L. A., & Mabury, S. A. (2014). Identification of novel fluorinated surfactants in aqueous film forming foams and commercial surfactant concentrates. *Environmental Science & Technology*, 48(1), 121–129. <https://doi.org/10.1021/es403729e>
10. Dai, M., Yan, N., & Brusseau, M. L. (2023). Potential impact of bacteria on the transport of PFAS in porous media. *Water Research*, 243, 120350. <https://doi.org/10.1016/j.watres.2023.120350>
11. De Rijk, V., Buma, J., Veldkamp, H., & Zech, A. (2025). Predicting saturated hydraulic conductivity from particle size distributions using machine learning. *Stochastic Environmental Research and Risk Assessment*, 39(2), 423–435. <https://doi.org/10.1007/s00477-024-02861-6>
12. De Silva, A. O., Armitage, J. M., Bruton, T. A., Dassuncao, C., Heiger-Bernays, W., et al. (2020). PFAS exposure pathways for humans and wildlife: A synthesis of current knowledge and key gaps in understanding. *Environmental Toxicology and Chemistry*, 40(3), 631–657. <https://doi.org/10.1002/etc.4935>
13. Dupla, X., Gondret, K., Sauzet, O., Verrecchia, E., & Boivin, P. (2021). Changes in topsoil organic carbon content in the Swiss leman region cropland from 1993 to present. Insights from large scale on-farm study. *Geoderma*, 400, 115125. <https://doi.org/10.1016/j.geoderma.2021.115125>
14. Edmonds, D. A., Caldwell, R. L., Brondizio, E. S., & Siani, S. M. O. (2020). Coastal flooding will disproportionately impact people on river deltas. *Nature Communications*, 11(1), 4741. <https://doi.org/10.1038/s41467-020-18531-4>
15. Farias, C. B. B., Almeida, F. C. G., Silva, I. A., Souza, T. C., Meira, H. M., et al. (2021). Production of green surfactants: Market prospects. *Electronic Journal of Biotechnology*, 51, 28–39. <https://doi.org/10.1016/j.ejbt.2021.02.002>
16. Gnesda, W. R., Draxler, E. F., Tinjum, J., & Zahasky, C. (2022). Adsorption of PFAAs in the vadose zone and implications for long-term groundwater contamination. *Environmental Science & Technology*, 56(23), 16748–16758. <https://doi.org/10.1021/acs.est.2c03962>
17. Gudiña, E. J., Rodrigues, A. I., Alves, E., Domingues, M. R., Teixeira, J. A., & Rodrigues, L. R. (2015). Bioconversion of agro-industrial by-products in rhamnolipids toward applications in enhanced oil recovery and bioremediation. *Bioresource Technology*, 177, 87–93. <https://doi.org/10.1016/j.biortech.2014.11.069>

18. Guelfo, J. L., & Higgins, C. P. (2013). Subsurface transport potential of perfluoroalkyl acids at aqueous film-forming foam (AFFF)-impacted sites. *Environmental Science & Technology*, 47(9), 4164–4171. <https://doi.org/10.1021/es3048043>
19. Guo, B., & Brusseau, M. L. (2024). Challenges and opportunities for porous media research to address PFAS groundwater contamination. *InterPore Journal*, 1(2), ipj240824-2. <https://doi.org/10.69631/ipj.v1i2nr35>
20. Guo, B., Saleem, H., & Brusseau, M. L. (2023). Predicting interfacial tension and adsorption at fluid–fluid interfaces for mixtures of PFAS and/or hydrocarbon surfactants. *Environmental Science & Technology*, 57(21), 8044–8052. <https://doi.org/10.1021/acs.est.2c08601>
21. Guo, B., Zeng, J., & Brusseau, M. L. (2020). A mathematical model for the release, transport, and retention of per- and polyfluoroalkyl substances (PFAS) in the vadose zone. *Water Resources Research*, 56(2), e2019WR026667. <https://doi.org/10.1029/2019WR026667>
22. He, K., Feerick, A., Jin, H., Batista Andrade, J. A., Duarte Batista, M., et al. (2024). Retention of per- and polyfluoroalkyl substances by syringe filters. *Environmental Chemistry Letters*, 22(4), 1569–1579. <https://doi.org/10.1007/s10311-024-01718-2>
23. Helmy, Q., Gustiani, S., & Mustikawati, A. (2020). Application of rhamnolipid biosurfactant for bio-detergent formulation. *IOP Conference Series: Materials Science and Engineering*, 823(1), 012014. <https://doi.org/10.1088/1757-899X/823/1/012014>
24. Høisæter, Å., Pfaff, A., & Breedveld, G. D. (2019). Leaching and transport of PFAS from aqueous film-forming foam (AFFF) in the unsaturated soil at a firefighting training facility under cold climatic conditions. *Journal of Contaminant Hydrology*, 222, 112–122. <https://doi.org/10.1016/j.jconhyd.2019.02.010>
25. Houtz, E. F., Higgins, C. P., Field, J. A., & Sedlak, D. L. (2013). Persistence of perfluoroalkyl acid precursors in AFFF-impacted groundwater and soil. *Environmental Science & Technology*, 47(15), 8187–8195. <https://doi.org/10.1021/es4018877>
26. Hu, X. C., Andrews, D. Q., Lindstrom, A. B., Bruton, T. A., Schaidler, L. A., et al. (2016). Detection of poly- and perfluoroalkyl substances (PFASs) in U.S. Drinking water linked to industrial sites, military fire training areas, and wastewater treatment plants. *Environmental Science & Technology Letters*, 3(10), 344–350. <https://doi.org/10.1021/acs.estlett.6b00260>
27. Huang, D., Saleem, H., Guo, B., & Brusseau, M. L. (2022). The impact of multiple-component PFAS solutions on fluid–fluid interfacial adsorption and transport of PFOS in unsaturated porous media. *Science of The Total Environment*, 806, 150595. <https://doi.org/10.1016/j.scitotenv.2021.150595>
28. ISO. (2019). ISO 21268-3:2019. Soil Quality - Leaching Procedures for Subsequent Chemical and Ecotoxicological Testing of Soil and Soil-Like Materials - Part 3: Up-flow Percolation Test. International Organization for Standardization. <https://www.iso.org/standard/68252.html>
29. ITRC. (2018). Environmental Fate and Transport for Per- and Polyfluoroalkyl Substances. PFAS Fact Sheets 5. Interstate Technology Regulatory Council. https://www.google.com/url?sa=t&source=web&rct=j&opi=89978449&url=https://documents.dps.ny.gov/public/Common/ViewDoc.aspx%3FDocRefId%3D%257B5BA26C14-0AA1-4A81-A04F-7D40DC33595B%257D&ved=2ahUKewjptPXN_6iQAxXv-AIHhBp6EQcQFnoECBoQAQ&usq=AOvVaw3-fSnVcC0XtmFFEhixZqBC
30. ITRC. (2023 September). Sampling Precautions and Laboratory Analytical Methods for Per- and Polyfluoroalkyl Substances (PFAS). PFAS Fact Sheets. Interstate Technology Regulatory Council. https://pfas-1.itrcweb.org/wp-content/uploads/2022/09/Sampling_and_Lab_PFAS_Fact-Sheet_082522_508.pdf
31. Ji, Y., Yan, N., Brusseau, M. L., Guo, B., Zheng, X., et al. (2021). Impact of a hydrocarbon surfactant on the retention and transport of perfluorooctanoic acid in saturated and unsaturated porous media. *Environmental Science & Technology*, 55(15), 10480–10490. <https://doi.org/10.1021/acs.est.1c01919>
32. Kabiri, S., Tucker, W., Navarro, D. A., Bräunig, J., Thompson, K., et al. (2022). Comparing the leaching behavior of per- and polyfluoroalkyl substances from contaminated soils using static and column leaching tests. *Environmental Science & Technology*, 56(1), 368–378. <https://doi.org/10.1021/acs.est.1c06604>
33. Krumina, L., Kenney, J. P. L., Loring, J. S., & Persson, P. (2016). Desorption mechanisms of phosphate from ferrihydrite and goethite surfaces. *Chemical Geology*, 427, 54–64. <https://doi.org/10.1016/j.chemgeo.2016.02.016>
34. Kuyukina, M. S., Ivshina, I. B., Makarov, S. O., Litvinenko, L. V., Cunningham, C. J., & Philp, J. C. (2005). Effect of biosurfactants on crude oil desorption and mobilization in a soil system. *Environment International*, 31(2), 155–161. <https://doi.org/10.1016/j.envint.2004.09.009>
35. Liao, S., Arshadi, M., Woodcock, M. J., Saleeba, Z. S. S. L., Pinchbeck, D., et al. (2022). Influence of residual nonaqueous-phase liquids (NAPLs) on the transport and retention of perfluoroalkyl substances. *Environmental Science & Technology*, 56(12), 7976–7985. <https://doi.org/10.1021/acs.est.2c00858>

36. Liu, M., Munoz, G., Vo Duy, S., Sauvé, S., & Liu, J. (2022). Per- and polyfluoroalkyl substances in contaminated soil and groundwater at airports: A Canadian case study. *Environmental Science & Technology*, 56(2), 885–895. <https://doi.org/10.1021/acs.est.1c04798>
37. Luft, C. M., Schutt, T. C., & Shukla, M. K. (2022). Properties and mechanisms for PFAS adsorption to aqueous clay and humic soil components. *Environmental Science & Technology*, 56(14), 10053–10061. <https://doi.org/10.1021/acs.est.2c00499>
38. Lyu, X., Li, Z., Wang, D., Zhang, Q., Gao, B., et al. (2022). Transport of perfluorooctanoic acid in unsaturated porous media mediated by SDBS. *Journal of Hydrology*, 607, 127479. <https://doi.org/10.1016/j.jhydrol.2022.127479>
39. Lyu, Y., & Brusseau, M. L. (2020). The influence of solution chemistry on air-water interfacial adsorption and transport of PFOA in unsaturated porous media. *Science of The Total Environment*, 713, 136744. <https://doi.org/10.1016/j.scitotenv.2020.136744>
40. Madsen, J. K., Pihl, R., Mller, A. H., Madsen, A. T., Otzen, D. E., & Andersen, K. K. (2015). The anionic biosurfactant rhamnolipid does not denature industrial enzymes. *Frontiers in Microbiology*, 6. <https://doi.org/10.3389/fmicb.2015.00292>
41. Maimaiti, A., Deng, S., Meng, P., Wang, W., Wang, B., et al. (2018). Competitive adsorption of perfluoroalkyl substances on anion exchange resins in simulated AFFF-impacted groundwater. *Chemical Engineering Journal*, 348, 494–502. <https://doi.org/10.1016/j.cej.2018.05.006>
42. Maizel, A. C., Shea, S., Nickerson, A., Schaefer, C., & Higgins, C. P. (2021). Release of per- and polyfluoroalkyl substances from aqueous film-forming foam impacted soils. *Environmental Science & Technology*, 55(21), 14617–14627. <https://doi.org/10.1021/acs.est.1c02871>
43. Naka, A., Yasutaka, T., Sakanakura, H., Kalbe, U., Watanabe, Y., et al. (2016). Column percolation test for contaminated soils: Key factors for standardization. *Journal of Hazardous Materials*, 320, 326–340. <https://doi.org/10.1016/j.jhazmat.2016.08.046>
44. *New risk limits for PFAS in surface water / RIVM*. (2022 September 26). National Institute for Public Health and the Environment. <https://www.rivm.nl/en/news/new-risk-limits-for-PFAS-in-surface-water>
45. Nguyen, T. T., Youssef, N. H., McInerney, M. J., & Sabatini, D. A. (2008). Rhamnolipid biosurfactant mixtures for environmental remediation. *Water Research*, 42(6–7), 1735–1743. <https://doi.org/10.1016/j.watres.2007.10.038>
46. Niarchos, G., Ahrens, L., Kleja, D. B., & Fagerlund, F. (2022). Per- and polyfluoroalkyl substance (PFAS) retention by colloidal activated carbon (CAC) using dynamic column experiments. *Environmental Pollution*, 308, 119667. <https://doi.org/10.1016/j.envpol.2022.119667>
47. Nickerson, A., Maizel, A. C., Schaefer, C. E., Ranville, J. F., & Higgins, C. P. (2023). Effect of geochemical conditions on PFAS release from AFFF-impacted saturated soil columns. *Environmental Science: Processes & Impacts*, 25(3), 405–414. <https://doi.org/10.1039/D2EM00367H>
48. Onaizi, S. A. (2018). Dynamic surface tension and adsorption mechanism of surfactin biosurfactant at the air–water interface. *European Biophysics Journal*, 47(6), 631–640. <https://doi.org/10.1007/s00249-018-1289-z>
49. Reijneveld, A., Van Wensem, J., & Oenema, O. (2009). Soil organic carbon contents of agricultural land in the Netherlands between 1984 and 2004. *Geoderma*, 152(3–4), 231–238. <https://doi.org/10.1016/j.geoderma.2009.06.007>
50. Senevirathna, S. T. M. L. D., Mahinroosta, R., Li, M., & Krishna Pillai, K. (2021). In situ soil flushing to remediate confined soil contaminated with PFOS- an innovative solution for emerging environmental issue. *Chemosphere*, 262, 127606. <https://doi.org/10.1016/j.chemosphere.2020.127606>
51. Shojaei, M., Kumar, N., Chaobol, S., Wu, K., Crimi, M., & Guelfo, J. (2021). Enhanced recovery of per- and polyfluoroalkyl substances (PFASs) from impacted soils using heat activated persulfate. *Environmental Science & Technology*, 55(14), 9805–9816. <https://doi.org/10.1021/acs.est.0c08069>
52. Simunek, J., M. van Genuchten, M. Sejna, N. Toride, and F. J. Leij. (1999). The STANMOD Computer Software for Evaluating Solute Transport in Porous Media Using Analytical Solutions of Convection-Dispersion Equation. Research (Report) IGWMC - TPS - 71. Golden, Colorado: International Ground Water Modeling Center, Colorado School of Mines. <https://www.pc-progress.com/Documents/Jirka/Stamod.pdf>
53. Smeck, Neil E. 1973. "Phosphorus: An Indicator of Pedogenetic Weathering Processes." *Soil Science* 115 (3): 199–206. https://journals.lww.com/soilsci/abstract/1973/03000/phosphorus__an_indicator_of_pedogenetic_weathering.5.aspx
54. Suhandono, S., Kusuma, S. H., & Meitha, K. (2021). Characterization and production of rhamnolipid biosurfactant in recombinant escherichia coli using autoinduction medium and palm oil mill effluent. *Brazilian Archives of Biology and Technology*, 64, e21200301. <https://doi.org/10.1590/1678-4324-2021200301>
55. Toride, N., F. J. Leij, and M. van Genuchten. (1995). The CXTFIT Code for Estimating Transport Parameters from Laboratory or Field Tracer Experiments. Research Report 137. Riverside, California: U.S. Salinity Lab., USDA, ARS. https://www.ars.usda.gov/arsuserfiles/20360500/pdf_pubs/P1444.pdf

56. Tsou, K., Antell, E., Duan, Y., Olivares, C. I., Yi, S., Alvarez-Cohen, L., & Sedlak, D. L. (2023). Improved total oxidizable precursor assay for quantifying polyfluorinated compounds amenable to oxidative conversion to perfluoroalkyl carboxylic acids. *ACS ES&T Water*, 3(9), 2996–3003. <https://doi.org/10.1021/acsestwater.3c00224>
57. US EPA. (2021 August). Draft Method 1633 analysis of per-and polyfluoroalkyl substances (PFAS) in aqueous, solid, biosolids, and tissue samples by LC-MS/MS. United States Environmental Protection Agency. https://www.epa.gov/system/files/documents/2021-09/method_1633_draft_aug-2021.pdf
58. US EPA. (2025 May 5). *SW-846 Test Method 1314: Liquid-solid Partitioning as a Function of Liquid-Solid Ratio for Constituents in Solid Materials Using an up-Flow Percolation Column Procedure*. United States Environmental Protection Agency. <https://www.epa.gov/hw-sw846/sw-846-test-method-1314-liquid-solid-partitioning-function-liquid-solid-ratio-constituents>
59. US EPA. (2022 December). *IRIS Toxicological Review of Perfluorobutanoic Acid (PFBA, CASRN 37522-4) and Related Salts*. EPA/635/R-22/277Fa. United States Environmental Protection Agency. <https://iris.epa.gov/static/pdfs/0701tr.pdf>
60. US EPA. (2024, November 26). *Our current understanding of the human health and environmental risks of PFAS* [Overviews and Factsheets]. <https://www.epa.gov/pfas/our-current-understanding-human-health-and-environmental-risks-pfas>
61. van Asseldonk, I. 2021. Nader Bodemonderzoek Blusplaats Munsterlaan Te Utrecht. [Further soil investigation at the Munsterlaan fire site in Utrecht]. Technical Report. 213044. BK Engineers, The Netherlands.
62. Van Glubt, S., & Brusseau, M. L. (2021). Contribution of nonaqueous-phase liquids to the retention and transport of per and polyfluoroalkyl substances (PFAS) in porous media. *Environmental Science & Technology*, 55(6), 3706–3715. <https://doi.org/10.1021/acs.est.0c07355>
63. Woudneh, M. B., Chandramouli, B., Hamilton, C., & Grace, R. (2019). Effect of sample storage on the quantitative determination of 29 PFAS: Observation of analyte interconversions during storage. *Environmental Science & Technology*, 53(21), 12576–12585. <https://doi.org/10.1021/acs.est.9b03859>
64. Yasutaka, T., Naka, A., Sakanakura, H., Kurosawa, A., Inui, T., et al. (2017). Reproducibility of up-flow column percolation tests for contaminated soils. *PLOS ONE*, 12(6), e0178979. <https://doi.org/10.1371/journal.pone.0178979>